Spatial Statistics 75 (2026) 101014

Contents lists available at ScienceDirect

Spatial Statistics

journal homepage: www.elsevier.com/locate/spasta

Constructing novel spatio-temporal difference-based covariance models[☆]

Sandra De Iaco [a,*], Donato Posa [b]

[a] Lecce, Italy
[b] University of Salento, Italy

ARTICLE INFO

Keywords:
Spectral density function
Correlation functions
Negative correlation

ABSTRACT

Data exhibiting negative correlation, particularly in temporal, spatial and spatio-temporal contexts, are frequently described by employing hole effect models or damped oscillation models. Nevertheless, these classical models suffer from severe limitations that reduce their adaptability. Specifically, models belonging to the Bessel class are criticised for consistently displaying a parabolic behaviour near the origin and an uncountable number of zeros. Furthermore, particular models within this class, such as the cosine model, suffer from additional drawbacks, including lack of admissibility in Euclidean spaces of dimension greater than one and not being strictly positive definite. Recently, wide classes of covariance functions, built through the difference of two correlation models, present distinct characteristics with respect to the traditional hole effect models and are considered to be sufficiently flexible, also in space–time. In this paper a further advance to construct correlation models, characterised by negative values, in a spatio-temporal domain is proposed as well as some examples and a case study are presented.

1. Introduction

Most of the spatial and spatio-temporal correlation functions presented in the scientific literature and applied in practice are non-negative; this characteristic is prominent across various fields, including meteorology, environmental sciences, machine learning and finance (Cressie and Huang, 1999; De Cesare et al., 2001; De Iaco et al., 2001; Gneiting, 2002b; Ma, 2002; Kolovos et al., 2004). A primary example is the widely-used Matérn class of covariance functions, which is inherently limited to modelling only non-negative correlation structures (Matérn, 1980). This represents a significant drawback, as it forecloses the possibility of modelling negative correlation, which is required in numerous applications concerning turbulence, hydrology, biology and demographic phenomena (Yaglom, 1955; Shkarofsky, 1968; Levinson et al., 1984; Yakhot et al., 1989; Pomeroy et al., 2003; Xu et al., 2003a,b; Posa et al., 2025).

Traditionally, negative correlation structures, often termed “hole effects” in mining and geological applications, are modelled using the Bessel family of covariance functions (Journel and Froidevaux, 1982; Ma and Jones, 2001; Asghari, 2015).

Hole effect models, beyond their traditional use in geology and mining, have also been applied in neuroscience to analyse the fluctuating spatial structure found in functional magnetic imaging (fMRI) data (Ye et al., 2015), which helps improve the accuracy of detecting areas in the brain that are activated during specific tasks. Furthermore, the same models have been utilised in environmental science for predicting and mapping the concentrations of airborne particulate matter (Alegria and Emery, 2024).

☆ This article is part of a Special issue entitled: ‘SPASTA_dawn of AI’ published in Spatial Statistics.
* Corresponding author.
E-mail address: sandra.deiaco@unisalento.it (S. De Iaco).

https://doi.org/10.1016/j.spasta.2026.101014
Received 23 November 2025; Received in revised form 22 June 2026; Accepted 23 June 2026

Available online 29 June 2026

However, these classical models present severe limitations that restrict their flexibility. Specifically, models from the Bessel class invariably exhibit a parabolic behaviour near the origin and are characterised by a countable infinity of zeros. Furthermore, particular models within this class, such as the cosine model, suffer from additional drawbacks, including lack of admissibility in Euclidean spaces of dimension greater than one and not being strictly positive definite (Chilès and Delfiner, 1999; De Iaco and Posa, 2018).

The literature has explored several avenues to overcome these limitations. These include linear combinations of covariance functions with negative weights (Vecchia, 1988; Ma, 2005; Gregori et al., 2008), compactly supported functions designed to model negative correlations (Gneiting, 2002a) and specialised models with negative "holes" (Hristopulos and Elogne, 2007). More recent contributions include new parametric families of isotropic matrix-valued functions with non-monotonic behaviours (Alegria and Emery, 2024), a comprehensive analysis of covariance functions exhibiting geometric anisotropies (Alegria and Emery, 2026) and the examination of spectral densities with a maximum not located at zero frequency.

A significant advance was achieved by constructing flexible classes of covariance functions through the difference of two correlation models, particularly from the Matérn family (Posa, 2021, 2025a). Moreover, through the spectral representation, a generalisation of the Cauchy family and a generalisation of a subclass of the Matérn family were constructed (Posa, 2025c). All these new families are exceptionally versatile; indeed, depending on their parameter values, a relevant property of these new classes regards their ability to model both exclusively positive and mixed positive–negative correlation within the same parametric family, a flexibility that most well-known covariance functions lack. Furthermore, they exhibit a complementary behaviour compared to the traditional Bessel class: they are essentially characterised by just one zero and can describe a linear behaviour near the origin, a feature that the entire class of Bessel models cannot capture. Moreover, an extension to families of correlation functions to be valid in Euclidean spaces of any dimension with further peculiar properties, was established (De Iaco and Posa, 2025).

In addition to using the classical Bochner's spectral representation, another technique to obtain negative correlation structures through differentiation of classical, always-positive covariance functions was provided. This approach leads to a remarkable and innovative result: the construction of covariance classes which present a finite countable set of zeros (Posa, 2025b). It also allows for the construction of valid classes of covariance functions which present a negative correlation even when the initial models are strictly positive. A peculiar contribution which enriches several traditional classes of covariance functions in a spatio-temporal context appeared in Posa (2023a), where some classes of separable and non-separable models which present negative correlation were provided and, moreover, the concept of separability was properly generalised. These achievements were of significant interest from both a theoretical and practical standpoint. From the last point of view, they provided a valuable guide for practitioners on how to use covariance functions which present negative values, taking into account crucial characteristics related to the spatial dimension, to the behaviour in proximity of the origin, as well as to the number of zeros.

Taking into account the previous studies, the aim of the present manuscript is to provide further advances for the class of spatio-temporal covariance functions with a negative correlation. Specifically, a general result derived through partial Fourier transform is given and the difference between models of the Gneiting class is analysed. They represent a substantial progress with respect to the existing families of covariance models. Surely, modelling spatial and spatial–temporal covariance functions is still crucial in the Artificial Intelligence epoch, since covariance models act as a bridge between geostatistics and modern ML kernel theory (De Iaco et al., 2022; Lan, 2022). Indeed, they represent valid kernel functions, making them directly usable in Support Vector Machine (SVMs), Kernel Ridge Regression, Spectral and manifold learning techniques, to encode spatial dependence directly into the learning algorithm. In this context, they can support the nonlinear modelling without explicitly mapping data to high dimensions, incorporating spatial smoothness assumptions and controlling model complexity through kernel hyperparameters. Other contributions on deep networks do not explicitly define covariance functions, but spatial or spatial–temporal covariance ideas appear implicitly (Nag et al., 2023; Wikle and Zammit-Mangion, 2023; Wang et al., 2025). Moreover, covariance functions are the backbone of Gaussian Process (GP) models, which are widely used for capturing smooth spatial trends, quantifying predictive uncertainty or performing well with small datasets (Rasmussen and Williams, 2005). It is worth recalling that covariance functions are central to Kriging, which can be interpreted as a special case of Gaussian Process regression.

The main contents of the manuscript are summarised as follows. In Section 2, a brief theoretical framework, concerning the class of continuous spatio-temporal covariance functions obtained through the difference of two continuous families of covariance functions has been provided. In Sections 3 and 4, the original contributions have been presented: in particular, the former introduces the construction of new spatio-temporal classes of covariances based on partial Fourier transform, whereas the latter is focused on some innovative classes obtained through the differences between Gneiting covariance models. In Section 5 some extensions based on the product have been discussed, at last, in Section 6, a case study referred to a demographic variable, such as the internal migration rate, has been given.

2. A theoretical framework

A complete characterisation of continuous covariance functions is achieved through Bochner's theorem (Bochner, 1959). According to this theorem, a stationary, continuous, complex-valued function C, defined on $\mathbb{R}^d \times \mathbb{R}$, is a spatio-temporal covariance function if it is the Fourier transform of a non-negative function F that is both non-decreasing and finite, i.e.,

$$C(\mathbf{h}, u) = \int_{\mathbb{R}^d} \int_{\mathbb{R}} \exp[i(\boldsymbol{\omega}^T \mathbf{h} + \tau \cdot u)] dF(\boldsymbol{\omega}, \boldsymbol{\tau}). \tag{1}$$

where $\mathbf{h} \in \mathbb{R}^d$ and $u \in \mathbb{R}$ are the spatial and temporal lags, respectively.

A special characterisation of (1) outcomes from the absolute continuity of the function F, i.e.,

$$C(\mathbf{h},u)=\int_{\mathbb{R}^d}\int_{\mathbb{R}}\exp[i(\boldsymbol{\omega}^T\mathbf{h}+\tau\cdot u)]f(\boldsymbol{\omega},\tau)d\boldsymbol{\omega}d\tau, \tag{2}$$

where the spectral density f is such that $f(\boldsymbol{\omega},\tau)\geq 0,\boldsymbol{\omega}\in\mathbb{R}^d,\tau\in\mathbb{R}$ and $f\in L^1(\mathbb{R}^d\times\mathbb{R})$.

If $C\in L^1(\mathbb{R}^d\times\mathbb{R})$, then the spatio-temporal spectral density function is continuous, moreover:

$$f(\boldsymbol{\omega},\tau)=\int_{\mathbb{R}^d}\int_{\mathbb{R}}\exp[-i(\boldsymbol{\omega}^T\mathbf{h}+\tau\cdot u)]C(\mathbf{h},u)d\mathbf{h}du. \tag{3}$$

As clarified in Posa (2021), wider families of covariance functions can be obtained considering the difference of two classes of covariance functions on the basis of the Bochner's Theorem. The following result is easily specialised for the spatio-temporal context.

Theorem 2.1 (*Spatio-Temporal Difference*). *Let $C_k:\mathbb{R}^d\times\mathbb{R}\to\mathbb{C},k=1,2$, be covariance functions and consider*

$$C(\mathbf{h},u)=A\cdot C_1(\mathbf{h},u;\boldsymbol{\alpha})-B\cdot C_2(\mathbf{h},u;\boldsymbol{\beta}),\quad(\mathbf{h},u)\in\mathbb{R}^d\times\mathbb{R}, \tag{4}$$

where $\boldsymbol{\alpha}$ and $\boldsymbol{\beta}$ are vectors of parameters, $A>0,B>0$.

Let the covariance functions $C_k,k=1,2$, be as in (2), i.e.,

$$C_1(\mathbf{h},u;\boldsymbol{\alpha})=\int_{\mathbb{R}^d}\int_{\mathbb{R}}\exp[i(\boldsymbol{\omega}^T\mathbf{h}+\tau\cdot u)]f_1(\boldsymbol{\omega},\tau;\boldsymbol{\alpha})d\boldsymbol{\omega}d\tau,$$

$$C_2(\mathbf{h},u;\boldsymbol{\beta})=\int_{\mathbb{R}^d}\int_{\mathbb{R}}\exp[i(\boldsymbol{\omega}^T\mathbf{h}+\tau\cdot u)]f_2(\boldsymbol{\omega},\tau;\boldsymbol{\beta})d\boldsymbol{\omega}d\tau,$$

with $f_i(\boldsymbol{\omega},\tau;\cdot)\geq 0,\forall(\boldsymbol{\omega},\tau)\in\mathbb{R}^d\times\mathbb{R}$ and $\int_{\mathbb{R}^d}\int_{\mathbb{R}}f_i(\boldsymbol{\omega},\tau;\cdot)d\boldsymbol{\omega}d\tau<\infty,i=1,2$, then

$$C(\mathbf{h},u)=\int_{\mathbb{R}^d}\int_{\mathbb{R}}\exp(i\boldsymbol{\omega}^T\mathbf{h}+i\tau\cdot u)[A\cdot f_1(\boldsymbol{\omega},\tau;\boldsymbol{\alpha})-B\cdot f_2(\boldsymbol{\omega},\tau;\boldsymbol{\beta})]d\boldsymbol{\omega} \tag{5}$$

is a covariance function if and only if $\forall(\boldsymbol{\omega},\tau)\in\mathbb{R}^d\times\mathbb{R}$,

$$A\cdot f_1(\boldsymbol{\omega},\tau;\boldsymbol{\alpha})-B\cdot f_2(\boldsymbol{\omega},\tau;\boldsymbol{\beta})\geq 0,\qquad\int_{\mathbb{R}^d}\int_{\mathbb{R}}[A\cdot f_1(\boldsymbol{\omega},\tau;\boldsymbol{\alpha})-B\cdot f_2(\boldsymbol{\omega},\tau;\boldsymbol{\beta})]d\boldsymbol{\omega}d\tau<+\infty. \tag{6}$$

Note that since f_1 and f_2 are integrable functions, then the integrability of $A_1f_1(\boldsymbol{\omega};\boldsymbol{\alpha})-A_2f_2(\boldsymbol{\omega};\boldsymbol{\beta})$ is always satisfied. Hence, the admissibility of the covariance model depends on the condition on the sign of the linear combination of f_1 and f_2 in (6).

As shown in De Iaco et al. (2026), these models possess desirable characteristics for practical applications, making them useful in various case studies. An extension of the class of isotropic spatio-temporal covariance functions can be also obtained by applying the theoretical results in Posa (2023a) summerised hereafter. It is worth highlighting that these models exhibit different behaviours in proximity of the origin and can be either strictly positive or partially negative, depending on their parameters values.

2.1. A summary on wider families of spatio-temporal covariance functions

It is recognised that most of the spatio-temporal correlation models employed in the literature are just characterised by positive values (Matérn, 1980; Cressie and Huang, 1999; De Iaco et al., 2001, 2002; Gneiting, 2002b; Rodrigues and Diggle, 2010; Porcu and Zastavnyi, 2011). In the following, a summary of the results given in Posa (2023a), concerning the construction of larger families of spatio-temporal separable and non-separable models with negative values, is provided hereafter.

2.1.1. Wider classes of separable spatio-temporal covariance functions

The following expression describes the class of separable spatio-temporal covariance models:

$$C(\mathbf{h},u)=\sigma^2\cdot\rho_S(\mathbf{h})\rho_T(u),$$

where ρ_S and ρ_T are the spatial and the temporal marginals, respectively, and are usually chosen among the families of positive correlation models. Wider and flexible classes of correlation models can be obtained by suitably selecting the same marginals correlation functions ρ_S and ρ_T. According to some recent results (Posa, 2025a,b), the spatial marginal can be constructed through the difference between two Matérn models ρ_1 and ρ_2, that is

$$\rho_S(\mathbf{h})=A_1\cdot\rho_1(\mathbf{h};\alpha_1)-A_2\cdot\rho_2(\mathbf{h};\beta_1),\quad A_1-A_2=1, \tag{7}$$

whereas the temporal marginal can be constructed either through the difference between two Matérn models ρ_3 and ρ_4, that is

$$\rho_T(u)=B_1\cdot\rho_3(u;\alpha_2)-B_2\cdot\rho_4(u;\beta_2),\quad B_1-B_2=1, \tag{8}$$

either through models which generalise the Cauchy class and a peculiar class of Matérn family, characterised by as many zeros as desired. This is an exclusive property with respect to the whole class of hole effect models (with a countable infinity of zeros), but also with respect to the recent difference based models (which present just one zero). Consequently, considering the analysis given in the previous references, the spatial and the temporal marginals can assume positive or negative values by suitably selecting the parameters values.

2.1.2. More general classes of non separable spatio-temporal covariance functions

Certain revised models, such as the product-sum and the Rodrigues and Diggle family, are uniquely capable of describing both positive and negative correlation structures. Conversely, other well-known models, including those by Cressie and Huang (1999) and the entire Gneiting class (Gneiting, 2002b), are fundamentally limited to exhibiting only positive correlation values.

- **Modified product-sum models**
  Starting from the product-sum covariance model (De Cesare et al., 2001; De Iaco et al., 2001), the alternative linear combination of the product and the sum models, as in Posa (2023a), is given below:

$$C(\mathbf{h}, u) = k_1 \cdot C_{S,1}(\mathbf{h})C_{T,1}(u) + k_2 \cdot C_{S,2}(\mathbf{h}) + k_3 \cdot C_{T,2}(u), \quad k_1 > 0, k_2 \geq 0, k_3 \geq 0, \tag{9}$$

  where $C_{S,i}$ and $C_{T,i}, i = 1, 2$ are spatial and temporal covariance function, respectively, without assuming $C_{S,1} = C_{S,2} = C_S$ and $C_{T,1} = C_{T,2} = C_T$.
  Two particular expressions of (9) are the following:

$$\rho(\mathbf{h}, u) = A \cdot \rho_{S,1}(\mathbf{h})\rho_{T,1}(u) + B \cdot \rho_{S,2}(\mathbf{h}), \quad A > 0, B > 0, A + B = 1, \tag{10}$$

$$\rho(\mathbf{h}, u) = A \cdot \rho_{S,1}(\mathbf{h})\rho_{T,1}(u) + B \cdot \rho_{T,2}(u), \quad A > 0, B > 0, A + B = 1. \tag{11}$$

  These last models can present negative correlation values by properly selecting $\rho_{S,\cdot}$ and $\rho_{T,\cdot}$ as in (7) and in (8). Moreover, the temporal marginal $\rho_{T,\cdot}$, as specified in the previous section, can be chosen through the generalised expressions belonging to the Cauchy or to the subclass of Matérn class, but also considering strictly positive differentiable covariance functions, as previously underlined.
  The classes (10) and (11) show relevant characteristics; indeed, if either the spatial correlation function, or the temporal one are integrable, then for the family in (10):

$$\forall\, u, \lim_{\|\mathbf{h}\| \to \infty} \rho(\mathbf{h}, u) = 0; \qquad \forall\, \mathbf{h}, \lim_{|u| \to \infty} \rho(\mathbf{h}, u) = B\rho_{S,2}(\mathbf{h}),$$

  as well as for the family in (11):

$$\forall\, u, \lim_{\|\mathbf{h}\| \to \infty} \rho(\mathbf{h}, u) = B\rho_{T,2}(u); \qquad \forall\, \mathbf{h}, \lim_{|u| \to \infty} \rho(\mathbf{h}, u) = 0.$$

- **Modified Rodrigues and Diggle models**
  Posa (2023a) modified the original model proposed by Rodrigues and Diggle (2010), where all correlation functions were assumed to be positive, introducing a revised version that allows the integrable correlation functions $\rho_{S,1}, \rho_{S,2}, \rho_{T,1}$ and $\rho_{T,2}$ to assume positive or negative values, i.e.:

$$\rho(\mathbf{h}, u) = A \cdot \rho_{S,1}(\mathbf{h}; \boldsymbol{\theta}_1)\rho_{T,1}(u; \boldsymbol{\phi}_1) + B \cdot \rho_{S,2}(\mathbf{h}; \boldsymbol{\theta}_2)\rho_{T,2}(u; \boldsymbol{\phi}_2), \tag{12}$$

  with $A > 0, B > 0, A + B = 1$ and $\boldsymbol{\theta}_1, \boldsymbol{\phi}_1, \boldsymbol{\theta}_2, \boldsymbol{\phi}_2$ vectors of parameters. This modified class can be further expanded by removing the assumption of integrability for the correlation functions $\rho_{S,1}, \rho_{S,2}, \rho_{T,1}$ and $\rho_{T,2}$, so that it can be seen as a subclass of the generalised Rodrigues and Diggle models, provided that either $\rho_{S,2} = 1$ or $\rho_{T,2} = 1$ in (12).
- **Integrated product models**
  It has been underlined that the class in (9) is able to model negative correlation structures depending on the parameters chosen for their spatial and temporal marginals. Nevertheless, the integrated product models in a spatio-temporal context remain always positive, even when the marginal components may assume negative values. This result is further extended to the Cressie–Huang family, which is considered a particular class of the integrated product models.

3. Spatio-temporal classes of covariances based on partial Fourier inversion

The spatio-temporal classes of covariance functions based on the difference can be further enlarged with respect to the ones existing in the literature (Posa, 2023a). Admissibility conditions for new spatio-temporal non-separable difference-based covariance models are derived by using the Bochner's Theorem and the Fubini's Theorem. In particular, the following result is based on the partial Fourier inversion of a continuous, bounded, symmetric and integrable function.

Theorem 3.1. *Given the following function on* $\mathbb{R}^d \times \mathbb{R}$

$$C(\mathbf{h}, u) = A \cdot C_1(\mathbf{h}, u) - B \cdot C_2(\mathbf{h}, u), \tag{13}$$

where C_1 and C_2 are spatio-temporal continuous, bounded, symmetric and integrable functions, then $C(\mathbf{h}, u)$ is a spatio-temporal covariance function if and only if

$$C_{\boldsymbol{\omega}}(u) = A \cdot C_{1\boldsymbol{\omega}}(u) - B \cdot C_{2\boldsymbol{\omega}}(u) \tag{14}$$

is a covariance function for almost all $\boldsymbol{\omega} \in \mathbb{R}^d$, where $C_{k\boldsymbol{\omega}}(u)$, with $k = 1, 2$, are the d-variate Fourier transform of $C_k(\mathbf{h}, u)$, that is

$$C_{k\boldsymbol{\omega}}(u) = \int_{\mathbb{R}^d} e^{-i \cdot \mathbf{h}^T \boldsymbol{\omega}} C_k(\mathbf{h}, u) d\mathbf{h}, \qquad u \in R, \qquad k = 1, 2. \tag{15}$$

See the Appendix for the proof.

Note that it is common to adopt spatio-temporal covariance models which are isotropic only in space, that is $C(\mathbf{h}, u) = C(\|\mathbf{h}\|, u)$ thus the following result can be introduced as a special case of Theorem 3.1.

To this aim, in the only isotropic spatial case, if

$$\int_0^\infty h^{d-1}|C(h)|dh < \infty, \quad d \in \mathbb{N},\, d \geq 2, \tag{16}$$

where $h = \|\boldsymbol{h}\|$, then the spectral density of C exists. Moreover, the covariance can be expressed, as follows:

$$C(h) = \frac{2(\pi)^{d/2}}{\Gamma(d/2)} \int_0^\infty \Lambda_d(\omega h)\omega^{d-1} f(\omega)d\omega, \qquad h > 0, \tag{17}$$

and the corresponding spectral density f is obtained as specified below:

$$f(\omega) = \frac{1}{2^{d-1}(\pi)^{d/2}\Gamma(d/2)} \int_0^\infty \Lambda_d(\omega h)h^{d-1}C(h)dh, \qquad \omega \in \mathbb{R}, \tag{18}$$

where

$$\Lambda_d(\omega) = 2^{(d-2)/2}\Gamma(d/2)\frac{J_{(d-2)/2}(\omega)}{\omega^{(d-2)/2}},$$

and J is a Bessel function of order $(d-2)/2$.

As a consequence, given the Euclidean domain $\mathbb{R}^d \times \mathbb{R}$, the admissibility condition of $C(\mathbf{h}, u) = C(\|\mathbf{h}\|, u)$ to be a covariance function, isotropic in space, requires to compute the function $C_\omega(u)$ as in (18), that is

$$C_\omega(u) = \frac{1}{2^{d-1}(\pi)^{d/2}\Gamma(d/2)} \int_0^\infty \Lambda_d(\omega h)h^{d-1}C(h,u)dh, \qquad \omega \in \mathbb{R}, \tag{19}$$

and if it is finite, check that the same function C_ω is a covariance function for almost all ω.

Thus, Theorem 2.1 can be formulated for the covariance function $C(\mathbf{h}, u) = C(\|\mathbf{h}\|, u)$, as stated in the following Corollary.

Corollary 3.1. *Let $C_k : \mathbb{R}^d \times \mathbb{R} \to \mathbb{R}, k = 1, 2$, be covariance functions, which are isotropic in space, such that, for any u,*

$$C_k(h,u) = \frac{2(\pi)^{d/2}}{\Gamma(d/2)} \int_0^\infty \Lambda_d(\omega h)\omega^{d-1} C_{k\omega}(u)d\omega, \qquad h > 0, \qquad k = 1, 2,$$

where $C_k(h, u)$, for any u, satisfies the condition in (16). The function $C(h, u) = A \cdot C_1(h, u) - B \cdot C_2(h, u)$ is a covariance function if and only if

$$A \cdot C_{1\omega}(u) - B \cdot C_{2\omega}(u) \tag{20}$$

is a covariance function for almost all $\omega \in \mathbb{R}$, where $C_{k\omega}(u)$, with $k = 1, 2$, are of the form

$$C_{k\omega}(u) = \frac{1}{2^{d-1}(\pi)^{d/2}\Gamma(d/2)} \int_0^\infty \Lambda_d(\omega h)h^{d-1}C_k(h,u)dh, \qquad \omega \in \mathbb{R}. \tag{21}$$

In the following, new families of spatio-temporal covariance models on the Euclidean space $\mathbb{R}^d \times \mathbb{R}$ are provided, as well as a discussion on some analytical features.

4. Differences between Gneiting covariance models

In this section, some new classes of spatio-temporal models obtained through the difference of the Gneiting covariance families, assumed isotropic in space, are presented.

Corollary 4.1. *Given the Gneiting class of models, isotropic in space and defined as follows:*

$$C_G(h,u) = \frac{1}{[\psi(u^2)]^{d/2}}\,\phi\left(\frac{h^2}{\psi(u^2)}\right), \tag{22}$$

where $\phi(t), t \geq 0$, is a completely monotone function and $\psi(t), t \geq 0$ is a positive function with completely monotone derivative, let C be defined as follows:

$$C(h,u) = A \cdot C_{G_1}(h,u) - B \cdot C_{G_2}(h,u), \tag{23}$$

where C_{G_1} and C_{G_2} are spatio-temporal covariance models of type (22), characterised by the functions $\phi_1(t)$, $\psi_1(t)$ and $\phi_2(t)$, $\psi_2(t)$, respectively. If $C_{1\omega}(u)$ and $C_{2\omega}(u)$, as in (21), exist, that is

$$C_{k\omega}(u) = \frac{1}{2^{d-1}(\pi)^{d/2}\Gamma(d/2)} \int_0^\infty \Lambda_d(\omega h)h^{d-1}C_k(h,u)dh = \frac{1}{[\psi_k(u^2)]^{d/2}} f_{\phi_k}[\omega, \psi_k(u^2)],$$

where $f_{\phi_k}[\omega,\psi(u^2)]$ *is the spectral density of* $\phi_k[\cdot;\psi(u^2)], \quad k=1,2$, *then, the weighted difference function in (23) is a covariance function if and only if*

$$C_\omega(u) = A\cdot\frac{1}{[\psi_1(u^2)]^{d/2}}\, f_{\phi_1}[\omega,\psi_1(u^2)] - B\cdot\frac{1}{[\psi_2(u^2)]^{d/2}}\, f_{\phi_2}[\omega,\psi_2(u^2)], \tag{24}$$

is a covariance function for almost all ω.

The admissibility condition can be explored by means of a parametric study of the function in (24) for fixed functions ψ and ϕ. Note that the condition that $C_{1\omega}(u)$ and $C_{2\omega}(u)$ exist, is equivalent to the assumption made for the Cressie–Huang covariance models (Cressie and Huang, 1999), mentioned in Theorem 1 in Gneiting et al. (2001).

If the Matérn family is chosen among the completely monotone functions ϕ, the Gneiting covariance class in (22) can be specifically written as

$$C_M(h,u) = \frac{1}{[\psi(u^2)]^{d/2}2^{\nu-1}\Gamma(\nu)}\left(\frac{\lambda h}{\sqrt{\psi(u^2)}}\right)^{\nu} K_\nu\left(\frac{\lambda h}{\sqrt{\psi(u^2)}}\right), \tag{25}$$

with $\nu>0$ and $\lambda>0$.

Given $\lambda'(u) = \dfrac{\lambda}{\sqrt{\psi(u^2)}}$, its corresponding behaviour depends on ψ, which is a positive function with completely monotone derivative, thus it is an increasing function. The admissibility conditions of the weighted difference in (23) can be derived, by means of a parametric study, from the ones given on the difference of Matérn families in Posa (2025a).

4.1. Spatial exponential marginal

By selecting the rational model for the function ψ and the generalised exponential for the function ϕ, the following family of Gneiting covariance models on $\mathbb{R}^d\times\mathbb{R}$ is obtained

$$C_G(h,u) = \frac{1}{(a|u|^{2\alpha}+1)^{\beta d/2}}\cdot exp\left(-\frac{c\,h^{2\gamma}}{(a|u|^{2\alpha}+1)^{\gamma\beta}}\right), \tag{26}$$

where $\alpha,\gamma\in]0,1]$ and $\beta\in[0,1]$.

Assuming a linear behaviour near the origin for the spatial marginal ($\gamma=0.5$), a parabolic behaviour for the temporal profile ($\alpha=1$) and the presence of interaction in space and time ($\beta=1$), then the specific family of Gneiting covariance models on $\mathbb{R}^d\times\mathbb{R}$ is given below:

$$C(h,u) = \frac{1}{(a|u|^2+1)^{d/2}}\cdot exp\left(-\frac{c\,h}{(a|u|^2+1)^{1/2}}\right). \tag{27}$$

It can be shown that the difference between two Gneiting classes as in (27) is an admissible spatio-temporal class of covariance functions under appropriate conditions on the parameters.

Theorem 4.1. *Given the weighted difference*

$$C(h,u) = A\cdot C_1(h,u) - B\cdot C_2(h,u), \tag{28}$$

where C_1 *and* C_2 *are spatio-temporal covariance models of type (27) on* $\mathbb{R}^2\times\mathbb{R}$ *(for* $d=2$*), with parameters* a_1,c_1 *and* a_2,c_2*, respectively, it is a class of covariance functions:*

- *for any* a_1,c_1 *and* a_2,c_2*, with* $a_1>a_2$ *and* $c_1\geq c_2$*, if*

$$1\leq\left(\frac{c_1}{c_2}\right)^2 < \frac{a_1}{a_2}\leq\frac{A}{B}, \tag{29}$$

- *for any* a_1,c_1 *and* a_2,c_2*, with* $a_1\geq a_2$ *and* $c_1\leq c_2$*, if*

$$1\leq\left(\frac{c_2}{c_1}\right)\left(\frac{a_1}{a_2}\right)\leq\frac{A}{B}. \tag{30}$$

See the Appendix for the proof.

Table 1 summarises the main characteristics of difference-based model in (27) and its marginals, with the behaviour near the origin and specification on the their sign.

In a spatio-temporal domain $\mathbb{R}^d\times\mathbb{R}$, for any spatial dimension d, the admissibility conditions can be generalised starting from the conditions given for the difference of Matérn families in Posa (2025a).

Note that, given the model in (28), where C_1 and C_2 are spatio-temporal covariance models of type (27) for $d=2$, that is

$$C(h,u) = \frac{A}{(a_1|u|^2+1)}\cdot exp\left(-\frac{c_1\,h}{(a_1|u|^2+1)^{1/2}}\right) - \frac{B}{(a_2|u|^2+1)}\cdot exp\left(-\frac{c_2\,h}{(a_2|u|^2+1)^{1/2}}\right), \tag{31}$$

Table 1
Admissibility and properties of the difference-based Gneiting covariance models, with a spatial exponential marginal (n.o. stands for near the origin).

Admissibility in $\mathbb{R}^2 \times \mathbb{R}$		$1 \leq \left(\frac{c_1}{c_2}\right)^2 < \frac{a_1}{a_2} \leq \frac{A}{B}$ for $a_1 > a_2$ and $c_1 \geq c_2$	or	$1 \leq \left(\frac{c_2}{c_1}\right)\left(\frac{a_1}{a_2}\right) \leq \frac{A}{B}$ for $a_1 \geq a_2$ and $c_1 \leq c_2$
Necessary conditions for the marginals in				
		$\mathbb{R}^2$ (space)		$\mathbb{R}$ (time)
$1 \leq \frac{c_2}{c_1} < \frac{A}{B}$ Positive and Linear n.o.	or	$1 \leq \frac{c_1}{c_2} < \left(\frac{A}{B}\right)^{1/2}$ Negative and Linear n.o.		$1 \leq \frac{a_1}{a_2} \leq \left(\frac{A}{B}\right)^2$ Positive and Parabolic n.o.

the marginals in space and time are defined, respectively, as follows:

$$C(h,0) = A \cdot exp\left(-c_1\, h\right) - B \cdot exp\left(-c_2\, h\right), \tag{32}$$

$$C(0,u) = \frac{A}{(a_1|u|^2+1)} - \frac{B}{(a_2|u|^2+1)}, \tag{33}$$

which can be characterised by the same properties, in terms of behaviour near the origin and presence of negative values, already discussed in Posa (2023b), De Iaco and Posa (2025).

A graphical representation of the spatio-temporal covariance surface in (31) and its marginals is given in Fig. 1. It is worth pointing out the linear behaviour near the origin for the spatial marginal and the parabolic behaviour for the temporal one. As illustrated, this model can reproduce the presence of negative correlation values characterising especially the spatial profile.

4.2. Spatial Gaussian marginal

Starting from the model in (26) and assuming a parabolic behaviour near the origin for both the spatial marginal ($\gamma = 1$) and the temporal profile ($\alpha = 1$), with interaction parameter $\beta = 1$, then the specific family of Gneiting covariance models on $\mathbb{R}^d \times \mathbb{R}$ is given below:

$$C(h,u) = \frac{1}{(a|u|^2+1)^{d/2}} \cdot exp\left(-\frac{c\, h^2}{(a|u|^2+1)}\right). \tag{34}$$

Under suitable parameter constraints, the difference between two Gneiting classes of the form (34) defines a valid spatio-temporal covariance class.

Theorem 4.2. *Given the weighted difference*

$$C(h,u) = A \cdot C_1(h,u) - B \cdot C_2(h,u), \tag{35}$$

where C_1 and C_2 are spatio-temporal covariance models of type (34), with parameters a_1, c_1 and a_2, c_2, respectively, it is a class of covariance functions in $\mathbb{R}^d \times \mathbb{R}$,

- *when $a_1 > a_2$ and $c_1 > c_2$, if*
$$1 < \left(\frac{c_1}{c_2}\right)^d < \frac{a_1}{a_2}\left(\frac{c_1}{c_2}\right)^{d-1} < \left(\frac{A}{B}\right)^2; \tag{36}$$
- *when $a_1 \geq a_2$ and $c_1 = c_2$, if*
$$1 \leq \frac{a_1}{a_2} \leq \left(\frac{A}{B}\right)^2.$$

See the Appendix for the proof.

From the weighted difference in (35), where C_1 and C_2 are spatio-temporal covariance models of type (34), that is

$$C(h,u) = \frac{A}{(a_1|u|^2+1)^{d/2}} \cdot exp\left(-\frac{c_1\, h^2}{(a_1|u|^2+1)}\right) - \frac{B}{(a_2|u|^2+1)^{d/2}} \cdot exp\left(-\frac{c_2\, h^2}{(a_2|u|^2+1)}\right), \tag{37}$$

the marginals in space and time are defined below:

$$C(h,0) = A \cdot exp\left(-c_1\, h^2\right) - B \cdot exp\left(-c_2\, h^2\right), \tag{38}$$

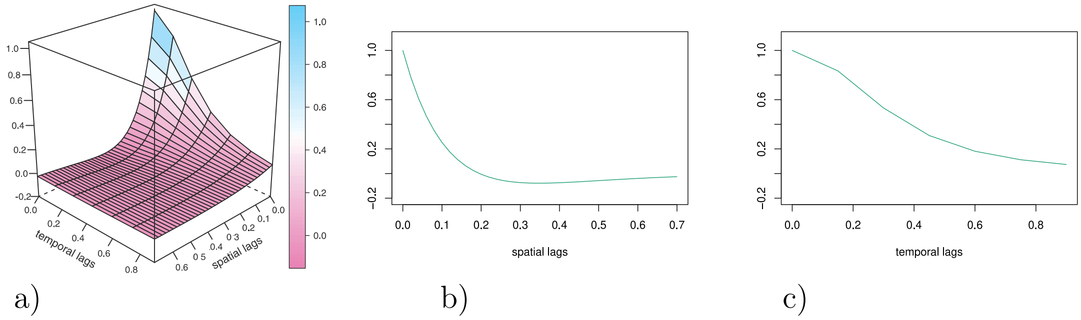

Fig. 1. (a) Spatio-temporal covariance model, based on the difference of non-separable Gneiting models, as in (31), with its (b) spatial and (c) temporal marginals, where $A = 6.9, B = 5.9, a_1 = 5, a_2 = 4.4, c_1 = 7, c_2 = 6.2$.

Table 2
Admissibility and properties of the difference-based Gneiting covariance models, with a spatial Gaussian marginal (n.o. stands for near the origin)

Admissibility in		
$\mathbb{R}^2 \times \mathbb{R}$	$1 < \left(\frac{c_1}{c_2}\right)^d < \frac{a_1}{a_2}\left(\frac{c_1}{c_2}\right)^{d-1} < \left(\frac{A}{B}\right)^2$ for $a_1 > a_2,\ c_1 > c_2$	or $1 \leq \frac{a_1}{a_2} \leq \left(\frac{A}{B}\right)^2$ for $a_1 \geq a_2,\ c_1 = c_2$
Necessary conditions for the marginals in	$\mathbb{R}^d$ (space)	$\mathbb{R}$ (time)
	$1 \leq \frac{c_1}{c_2} \leq \left(\frac{A}{B}\right)^{2/d}$	$1 \leq \frac{a_1}{a_2} \leq \left(\frac{A}{B}\right)^2$
	Negative and Parabolic n.o.	Positive and Parabolic n.o.

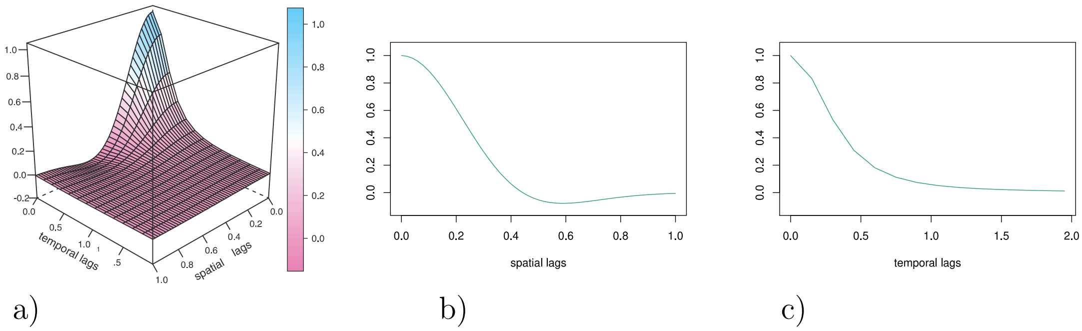

Fig. 2. (a) Spatio-temporal covariance model, based on the difference of non-separable Gneiting models, as in (37), with its (b) spatial and (c) temporal marginals, where $A = 6.9, B = 5.9, a_1 = 5, a_2 = 4.4, c_1 = 7, c_2 = 6.2$.

$$C(0,u) = \frac{A}{(a_1|u|^2+1)^{d/2}} - \frac{B}{(a_2|u|^2+1)^{d/2}}, \tag{39}$$

which have the same properties, in terms of behaviour near the origin and presence of negative values, already discussed in Posa (2023b), De Iaco and Posa (2025). In Table 2, the main features of difference-based model in (37) and its marginals, together with the behaviour near the origin and specification on the their sign are given.

A graphical representation of the spatio-temporal covariance surface in (37) and its marginals is given in Fig. 2. This covariance model has a parabolic behaviour near the origin for both the spatial and temporal marginals, typical of a phenomenon with a highly regular spatio-temporal evolution. The covariance surface shows a lower minimum value with respect to the model in Fig. 1, taking into account that the difference of isotropic Gaussian covariance functions, in $\mathbb{R}^d$ can reach the value -0.1355 for $d = 2$ (bi-dimensional spatial domain). If the coordinates h and u are swapped with each other in the model, then the corresponding temporal marginal, defined as difference of isotropic Gaussian covariance functions with $d = 1$, has an absolute minimum equal to -0.4453.

4.3. Computational remarks

Model fitting can be supported by using the R package `nloptr` implemented for nonlinear optimisation (Johnson, 2007). It requires the definition of the loss function and the constraints on the parameters. The fitting procedure can start from computing the optimal scaling parameter estimates for the sample marginals and then proceed with the estimation of the difference weights by using the spatio-temporal empirical covariance surface.

The estimation procedure can follow the steps described below:

1. estimate A, B and the scaling parameters c_1, c_2 for the spatial marginal, under the necessary admissibility conditions in $\mathbb{R}^d$, then denote the estimates as $A^{*1}, B^{*1}, c_1^{*1}, c_2^{*1}$;
2. estimate A, B and the scaling parameters a_1, a_2 for the temporal marginal, under the necessary admissibility conditions in $\mathbb{R}$, by initialising A, B with the estimates A^{*1}, B^{*1}, then denote the estimates as $A^{*2}, B^{*2}, a_1^{*1}, a_2^{*1}$;
3. estimate A, B and the scaling parameters c_1, c_2 for the spatial marginal, by initialising A, B, c_1, c_2 with the estimates A^{*2}, B^{*2} and c_1^{*1}, c_2^{*1}, then denote the estimates as $A^{*3}, B^{*3}, c_1^{*2}, c_2^{*2}$;
4. do steps 2 and 3 and estimate iteratively A^{*i}, B^{*i} as well as $a_1^{*(i-2)}, a_2^{*(i-2)}, c_1^{*(i-1)}, c_2^{*(i-1)}$ on the temporal and spatial marginals, respectively, for each cycle i, until the differences between the estimates at stage i and the previous ones are less than a given small constant or they remain unchanged after the iteration;
5. estimate A, B as well as the spatial and temporal scaling parameters, under the necessary admissibility conditions in $\mathbb{R}^d \times \mathbb{R}$, by using the empirical spatio-temporal covariance surface and giving as starting inputs the pre A^{*i}, B^{*i} and $a_1^{*(i-2)}, a_2^{*(i-2)}, c_1^{*(i-1)}, c_2^{*(i-1)}$.

5. Some extensions based on the product

Starting from Theorem 3.1, new classes of spatio-temporal covariance functions, characterised by positive or negative values, can be obtained through the difference of product models.

Theorem 5.1. *Given the following function on $\mathbb{R}^d \times \mathbb{R}$*

$$C(\mathbf{h}, u) = A \cdot C_{S1}(\mathbf{h}) C_{T1}(u) - B \cdot C_{S2}(\mathbf{h}) C_{T2}(u), \tag{40}$$

where $C_1(\mathbf{h}, u) = C_{S1}(\mathbf{h}) C_{T1}(u)$ and $C_2(\mathbf{h}, u) = C_{S2}(\mathbf{h}) C_{T2}(u)$ are spatio-temporal continuous, bounded, symmetric and integrable functions, then $C(\mathbf{h}, u)$ is a spatio-temporal covariance function if and only if

$$C_{\boldsymbol{\omega}}(u) = A \cdot C_{T1}(u) C_{1\boldsymbol{\omega}}(u) - B \cdot C_{T2}(u) C_{2\boldsymbol{\omega}}(u) \tag{41}$$

is a covariance function for almost all $\boldsymbol{\omega} \in \mathbb{R}^d$, where $C_{k\boldsymbol{\omega}}(u)$, with $k = 1, 2$, are the d-variate Fourier transform of $C_k(\mathbf{h}, u)$, that is

$$C_{k\boldsymbol{\omega}}(u) = C_{Tk}(u) \int_{\mathbb{R}^d} e^{-i \cdot \mathbf{h}^T \boldsymbol{\omega}} C_{Sk}(\mathbf{h}) d\mathbf{h}, \qquad u \in R, \qquad k = 1, 2. \tag{42}$$

In the isotropic case for the spatial profile, the above results can be further specialised.

Corollary 5.1. *Let $C_k : \mathbb{R}^d \times \mathbb{R} \to \mathbb{R}, k = 1, 2$, be the product of isotropic covariance functions, $C_k(h, u) = C_{Sk}(h) C_{Tk}(u)$ such that, for any u,*

$$C_k(h, u) = \frac{2(\pi)^{d/2}}{\Gamma(d/2)} \int_0^\infty \Lambda_d(\omega h) \omega^{d-1} C_{Tk}(u) C_{k\omega}(u) d\omega, \qquad h > 0, \qquad k = 1, 2,$$

where $C_k(\cdot, u)$ satisfies the condition in (16). The function $C(h, u) = A \cdot C_{S1}(h) C_{T1}(u) - B \cdot C_{S2}(h) C_{T2}(u)$ is a covariance function if and only if

$$C_\omega(u) = A \cdot C_{T1}(u) C_{1\omega}(u) - B \cdot C_{T2}(u) C_{2\omega}(u) \tag{43}$$

is a covariance function for almost all $\omega \in \mathbb{R}$, where $C_{k\omega}(u)$, with $k = 1, 2$, are of the form

$$C_{k\omega}(u) = \frac{C_{Tk}(u)}{2^{d-1}(\pi)^{d/2}\Gamma(d/2)} \int_0^\infty \Lambda_d(\omega h) h^{d-1} C_{Sk}(h) dh, \qquad \omega \in \mathbb{R}. \tag{44}$$

Two specific examples, obtained by selecting some spatial and temporal marginals, can be easily provided.

Example 5.1. Given two product models, $C_1(h, u) = C_{S1}(h) C_{T1}(u)$ and $C_2(h, u) = C_{S2}(h) C_{T2}(u)$, where C_{S1} are C_{S2} are isotropic spatial rational covariance models with scale parameters a_1 and a_2, respectively, while C_{T1} and C_{T2} are temporal exponential covariance models, with scale parameters c_1 and c_2, respectively, then the function

$$C(h, u) = \frac{A}{(h^2 + a_1^2)^{(d+1)/2}} exp(-c_1 u) - \frac{B}{(h^2 + a_2^2)^{(d+1)/2}} exp(-c_2 u)$$

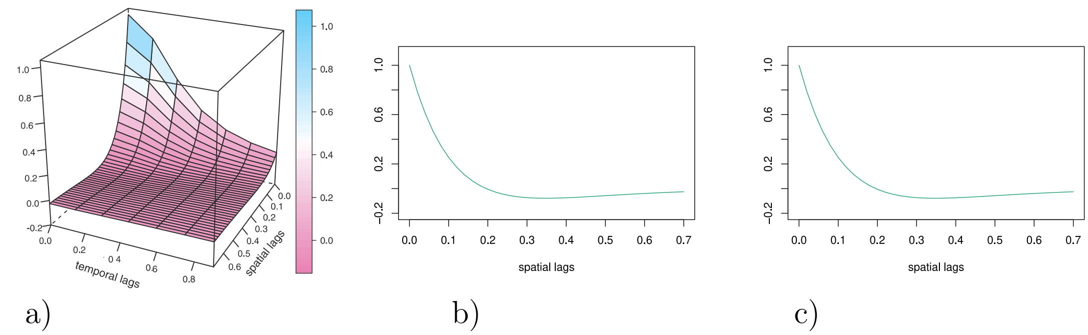

Fig. 3. (a) Spatio-temporal covariance model, based on the difference of separable models, as in (48), with its (b) spatial and (c) temporal marginals, where $A = 6.9, B = 5.9, a_1 = 5, a_2 = 4.4, c_1 = 7, c_2 = 6.2$.

is a covariance function if and only if

$$C_\omega(u) = A \cdot \left[W \cdot exp(-c_1\, u) \frac{\exp(-a_1\omega)}{a_1} \right] - B \cdot \left[W \cdot exp(-c_2\, u) \frac{\exp(-a_2\omega)}{a_2} \right], \tag{45}$$

where $W^{-1} = 2^d \pi^{(d-1)/2} \Gamma[(d+1)/2]$, is a covariance function for almost all $\omega \in \mathbb{R}$, that is, on the basis of the admissibility conditions in De Iaco and Posa (2025) if and only if

$$1 \leq \frac{c_2}{c_1} \leq \frac{A\, a_2}{B\, a_1} \cdot exp[\omega(a_2 - a_1)], \quad \text{or} \quad 1 \leq \frac{c_1}{c_2} \leq \left(\frac{A\, a_2}{B\, a_1} \cdot exp[\omega(a_2 - a_1)] \right)^{1/d}. \tag{46}$$

Thus, the condition is met for $a_2 > a_1$, when

$$\frac{a_1}{a_2} \leq \frac{c_2}{c_1}\frac{a_1}{a_2} \leq \frac{A}{B}, \quad \text{or} \quad \left(\frac{a_1}{a_2}\right)^{1/d} \leq \frac{c_1}{c_2}\left(\frac{a_1}{a_2}\right)^{1/d} \leq \frac{A}{B}. \tag{47}$$

If the rational model is used for the temporal marginal and the exponential for the spatial one, the following model

$$C(h,u) = \frac{A}{(u^2 + a_1^2)} \cdot exp(-c_1\, h) - \frac{B}{(u^2 + a_2^2)} \cdot exp(-c_2\, h), \tag{48}$$

is also admissible under the condition in (47) with $d = 1$. Fig. 3 provides a graphical representation of the above mentioned spatio-temporal covariance surface and its marginals. This model represents a special case of the model in (31), since it is just built through the difference of the product of the marginals in space and time of C_1 and C_2 in (31). Indeed, in this case, the spatio-temporal model is obtained through the weighted difference of separable models, while in (31) the corresponding spatio-temporal model is obtained through the difference of non-separable models. It is worth pointing out the linear behaviour near the origin for the spatial marginal and the parabolic behaviour for the temporal one. As illustrated, the spatio-temporal covariance surface can reproduce the presence of negative correlation values characterising especially the spatial profile.

Example 5.2. Given two product models, $C_1(h,u) = C_{S1}(h)C_{T1}(u)$ and $C_2(h,u) = C_{S2}(h)C_{T2}(u)$, where C_{S1} are C_{S2} are isotropic spatial Gaussian covariance models with scale parameters a_1 and a_2, respectively, while C_{T1} and C_{T2} are temporal exponential covariance models, with scale parameters c_1 and c_2, respectively, then the function

$$C(h,u) = A \cdot exp(-a_1\, h^2)\, exp(-c_1\, u) - B \cdot exp(-a_2\, h^2)\, exp(-c_2\, u)$$

is a covariance function if and only if

$$C_\omega(u) = A \cdot exp(-c_1\, u) \left(\frac{1}{4\pi a_1}\right)^{d/2} e^{-\omega^2/4a_1} - B \cdot exp(-c_2\, u) \left(\frac{1}{4\pi a_2}\right)^{d/2} e^{-\omega^2/4a_2}, \tag{49}$$

is a covariance function for almost all $\omega \in \mathbb{R}$, that is, on the basis of the admissibility conditions in De Iaco and Posa (2025) if and only if

$$1 \leq \frac{c_1}{c_2} \leq \left(\frac{A}{B}\right)^{2/d} \frac{a_2}{a_1} \cdot exp\left[\omega^2\left(\frac{1}{a_2} - \frac{1}{a_1}\right)\right]^{2/d}. \tag{50}$$

Thus, the condition is met for $a_1 > a_2$, when

$$\frac{a_1}{a_2} \leq \frac{c_1}{c_2}\frac{a_1}{a_2} \leq \left(\frac{A}{B}\right)^{2/d}. \tag{51}$$

Alternatively, other classes of spatio-temporal covariance functions, with positive or negative values, can be derived, on the basis of Theorem 3.1, from the product of difference of covariance models in space and time.

Theorem 5.2. *Given the following functions on $\mathbb{R}^d$ and on $\mathbb{R}$*

$$C_S(\mathbf{h}) = A_S \cdot C_{S1}(\mathbf{h}) - B_S \cdot C_{S2}(\mathbf{h}), \tag{52}$$

$$C_T(u) = A_T \cdot C_{T1}(u) - B_T \cdot C_{T2}(u), \tag{53}$$

where C_S and C_T are spatial and temporal continuous, bounded, symmetric and integrable functions, then $C(\mathbf{h}, u) = C_S(\mathbf{h})C_T(u)$ is a spatio-temporal covariance function if and only if $C_T(u)C_{S\boldsymbol{\omega}}(u)$ is a covariance function for almost all $\boldsymbol{\omega} \in \mathbb{R}^d$, where $C_{S\boldsymbol{\omega}}(u)$ is the d-variate Fourier transform of $C_k(\mathbf{h}, u)$, that is

$$C_{S\boldsymbol{\omega}}(u) = A_S \cdot \int_{\mathbb{R}^d} e^{-i\cdot\mathbf{h}^T\boldsymbol{\omega}} C_{S1}(\mathbf{h})d\mathbf{h} - B_S \cdot \int_{\mathbb{R}^d} e^{-i\cdot\mathbf{h}^T\boldsymbol{\omega}} C_{S2}(\mathbf{h})d\mathbf{h}, \qquad u \in R. \tag{54}$$

In case of spatial isotropy, the admissibility condition can be provided by recalling Corollary 3.1.

Corollary 5.2. *Let $C_S : \mathbb{R}^d \to \mathbb{R}$, and $C_T : \mathbb{R}^d \to \mathbb{R}$, be spatial and temporal isotropic difference-based covariance functions, respectively, then*

$$C(h, u) = C_S(h)C_T(u) = [A_S \cdot C_{S1}(h) - B_S \cdot C_{S2}(h)] \cdot [A_T \cdot C_{T_1}(u) - B_T \cdot C_{T_2}(u)], \tag{55}$$

such that, for any u,

$$C(h, u) = \frac{2(\pi)^{d/2}}{\Gamma(d/2)} C_T(u) \int_0^\infty \Lambda_d(\omega h)\omega^{d-1} C_{S\omega}(u)d\omega = \frac{2(\pi)^{d/2}}{\Gamma(d/2)} C_T(u) \int_0^\infty \Lambda_d(\omega h)\omega^{d-1} [A_S C_{S1\omega}(u) - B_S C_{S2\omega}(u)]d\omega,$$

where $C(\cdot, u)$ satisfies the condition in (16). The function $C(h, u)$ in (55) is a covariance function if and only if

$$C_\omega(u) = [A_S \cdot C_{S1\omega}(u) - B_S \cdot C_{S2\omega}(u)] \cdot [A_T \cdot C_{T_1}(u) - B_T \cdot C_{T_2}(u)] \tag{56}$$

is a covariance function for almost all $\omega \in \mathbb{R}$, where $C_{Sk\omega}(u)$, with $k = 1, 2$, are of the form

$$C_{Sk\omega}(u) = \frac{C_{Tk}(u)}{2^{d-1}(\pi)^{d/2}\Gamma(d/2)} \int_0^\infty \Lambda_d(\omega h)h^{d-1} C_{Sk}(h)dh, \qquad \omega \in \mathbb{R}. \tag{57}$$

The following example of class of spatio-temporal covariance models is proposed on the basis of the proposed construction.

Example 5.3. Given two isotropic difference models, $C_S(h) = A_S \cdot C_{S1}(h) - B_S \cdot C_{S2}(h)$ and $C_T(u) = A_T \cdot C_{T1}(u) - B_T \cdot C_{T2}(u)$, where C_{S1} are C_{S2} are spatial Gaussian covariance models with scale parameters a_1 and a_2, respectively, while C_{T1} and C_{T2} are temporal exponential covariance models, with scale parameters c_1 and c_2, respectively, then the product of the following functions

$$C_S(h) = A_S \cdot exp(-a_1\, h^2) - B_S \cdot exp(-a_2\, h^2)$$

$$C_T(u) = A_T \cdot exp(-c_1\, u) - B_T \cdot exp(-c_2\, u),$$

that is

$$C(h, u) = [A_S \cdot exp(-a_1\, h^2) - B_S \cdot exp(-a_2\, h^2)] \cdot [A_T \cdot exp(-c_1\, u) - B_T \cdot exp(-c_2\, u)],$$

is a covariance function if and only if

$$C_\omega(u) = \left[\left(\frac{A_S}{4\pi a_1}\right)^{d/2} \cdot e^{-\omega^2/4a_1} - \left(\frac{B_S}{4\pi a_2}\right)^{d/2} \cdot e^{-\omega^2/4a_2}\right] \left[A_T \cdot exp(-c_1\, u) - B_T \cdot exp(-c_2\, u)\right], \tag{58}$$

is a covariance function for almost all $\omega \in \mathbb{R}$. Thus, it is satisfied if

- the first factor is positive, that is
$$\left[\left(\frac{A_S}{4\pi a_1}\right)^{d/2} \cdot e^{-\omega^2/4a_1} - \left(\frac{B_S}{4\pi a_2}\right)^{d/2} \cdot e^{-\omega^2/4a_2}\right] > 0,$$
which implies that
$$1 < a_1/a_2 < (A_S/B_S)^{2/d}; \tag{59}$$
- $\left[A_T \cdot exp(-c_1\, u) - B_T \cdot exp(-c_2\, u)\right]$ is a temporal covariance (in one-dimensional domain), which implies that
$$1 \le \frac{c_2}{c_1} \le \frac{A_T}{B_T}, \quad \text{or} \quad 1 \le \frac{c_1}{c_2} \le \frac{A_T}{B_T}. \tag{60}$$

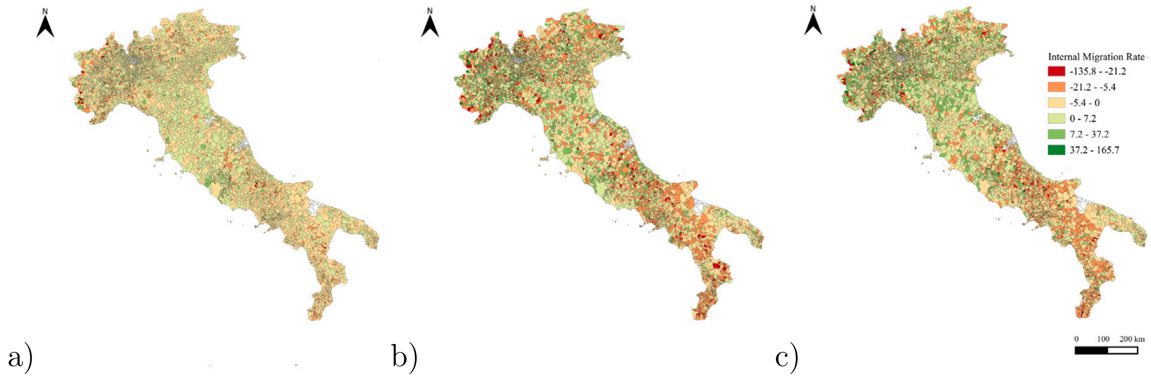

Fig. 4. Colour map of the IMR values, per 1000 inhabitants ($^o/_{oo}$), recorded in (a) 2001, (b) 2011, (c) 2021 at 7612 Italian municipalities.

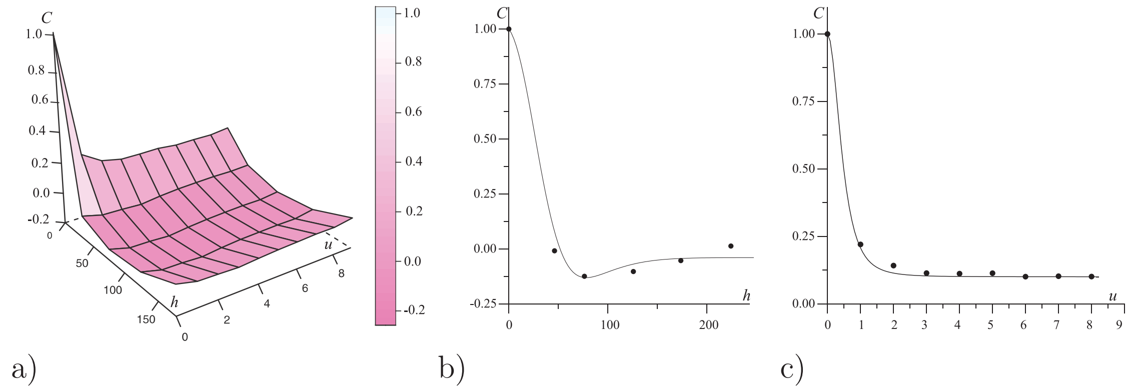

Fig. 5. (a) Sample spatio-temporal covariance function for the IMR (Italy), with (b) spatial and (c) temporal marginals, given in (64) and (65), together with their fitted models.

6. An application to a demographic variable

In the present section, the spatial observations of a demographic variable, provided by the Italian Institute of Statistics (ISTAT), have been analysed. The attention is focused on the Internal Migration Rate ($^o/_{oo}$) (IMR), which represents the net balance of internal mobility within Italy, calculated as the difference between arrivals and departures from/to other Italian municipalities, in relation to the average annual population.

6.1. Spatio-temporal data on IMR

The spatio-temporal dataset refers to the annual IMR averages ($^o/_{oo}$) observed at 7612 Italian municipalities over the period 2001–2021. Fig. 4 shows the spatial distribution of the variable of interest for three specific years, i.e. 2001, 2011 and 2021; thus, it highlights that values in the intermediate range are broadly distributed throughout the country. Apart from a few isolated municipalities that reach the highest rates, many other urban centres — including several provincial capitals — also exhibit relatively large IMRs, not only clustered around regional capitals. By contrast, the lowest IMR values are concentrated in the northern regions and in some scattered towns of the south-eastern area. Looking at the temporal evolution during the study period, lower values were registered in 2001, then an overall increase was shown in 2011 with a slight decrease in the last period. The lower internal migration rate observed in Italy around 2011 likely reflects a combination of cyclical and structural factors. The aftermath of the 2008–2010 global financial crisis and the subsequent European sovereign-debt recession depressed labour-market opportunities and housing turnover, reducing people's propensity to move. The stronger internal migration rates seen in more recent years are consistent with partial economic recovery, renewed labour mobility and changes in migration flows that increased the population segments most likely to move. The COVID-19 pandemic and the associated mobility restrictions produced a marked reduction in residential moves in 2020 (sharp monthly minima during lockdowns), which suppresses internal migration counts and affects the 2020–2021 observations; this explains part of the lower level seen around 2021 relative to the 2011 peak.

The assessment of the adequacy of the fitted model has been evaluated through the leave-one-out cross-validation procedure as well as the jackknife technique where different subsets of the available data have been used as validation sets. These jackknife subsets have been obtained by randomly selecting 30%, 40% and 50% spatio-temporal points (25,120 33,493 41,866, respectively) from the complete data set.

6.2. Estimation and modelling

This section focuses on the steps of the structural analysis, such as empirical covariance estimation, model fitting and model validation.

After estimating the spatio-temporal correlation function, the corresponding marginals in space and time have been analysed. In particular, the sample spatial covariance clearly shows decreasing values which are negative values until the sixth spatial lag, corresponding approximately to 170 km (Fig. 5-b) and the temporal marginal decays monotonically and gets stable around 0.1 (Fig. 5-c). On the basis of the inspection of the empirical features of the sample covariance function, it has been modelled through a linear combination of a purely spatial model, denoted with C_1 and the spatio-temporal model in (34), with $d = 2$, denoted with C_2. C_1 corresponds to the difference of spatial isotropic exponential models in order to better describe the rapid decline near the origin. On the other hand, C_2 has been described through the difference of Gneiting covariance functions, which can reproduce the depression in the covariance function, up to a minimum equal to -0.122. Consequently, the temporal profile has been modelled through the difference of two rational models, with a horizontal asymptote determined from the presence of a purely spatial structure in the spatio-temporal model. Thus, after the estimation of the parameters values by using the procedure in Section 4.3, the goodness of fit was assessed through standard deviation–derived indices.

Fig. 5 shows the sample spatio-temporal covariance function computed for 7 spatial lags and 8 temporal lags together with the marginals in space and time and the fitted model. Given the analytical expression of the selected spatio-temporal covariance model:

$$C(h,u) = 0.1 \cdot C_1(h) + 0.9 \cdot C_2(h,u), \tag{61}$$

where

$$C_1(h) = 1.3 \cdot \exp(-0.05\,h) - 0.3 \cdot \exp(-0.0245\,h) \tag{62}$$

$$C_2(h,u) = \frac{1.3}{3.597\,|u|^2+1} \cdot exp\left(-\frac{(0.025\,h)^2}{3.597\,|u|^2+1}\right) - \frac{0.3}{0.831\,|u|^2+1} \cdot exp\left(-\frac{(0.0121\,h)^2}{0.831\,|u|^2+1}\right), \tag{63}$$

the corresponding marginal in space is defined as:

$$C(h,0) = 0.1 \cdot \left[1.3 \cdot \exp(-0.05\,h) - 0.3 \cdot \exp(-0.0245\,h)\right] + 0.9\left[1.3 \cdot exp[-(0.025\,h)^2] - 0.3 \cdot exp[-(0.0121\,h)^2]\right] \tag{64}$$

where the first two exponential components decay approximately after 60 km (effective range given by 3/0.05) and 122 km (effective range given by 3/0.0245), respectively, and the last two Gaussian components decay approximately after 70 km (effective range given by $\sqrt{3}/0.025$) and 145 km (effective range given by $\sqrt{3}/0.012$), respectively; while the marginal in time is:

$$C(0,u) = 0.1 + 0.9 \cdot \left[\frac{1.3}{3.597\,|u|^2+1} - \frac{0.3}{0.831\,|u|^2+1}\right], \tag{65}$$

where the two rational components decay approximately after 2 years and 6 years, respectively. Note the horizontal asymptote of the temporal marginal, is derived from the presence of a purely spatial structure in the spatio-temporal model. It is also worth pointing out that the parameters values satisfy the admissibility conditions already discussed in De Iaco and Posa (2025) and the one given in (36) for the part modelled through the difference of Gneiting covariance functions.

The empirical covariance is well represented by the selected spatio-temporal model, as confirmed by the mean deviation and the mean square deviation between the sample and the theoretical covariance surfaces, which are around 0.0125 and 0.0151, respectively. The model's predictive accuracy is confirmed by low cross-validation error rates: the relative (absolute and squared) error indices are 0.039 and 0.043, respectively. Using a jackknife procedure on a validation subset comprising 30% of units selected at random, the corresponding indices rise modestly to 0.072 and 0.083. These results indicate robust estimation performance and stable generalisation to unseen data, supporting the model's reliability for inference and prediction.

For comparative purposes, the non-separable covariance model $C_2(h,u)$ in (61) has been alternatively substituted with a separable model, based on the product of two difference models, one for the spatial marginal and the other one for the temporal marginal; hence, the spatio-temporal covariance model can be explicitly written as follows:

$$C(h,u) = 0.1 \cdot C_1(h) + 0.9 \cdot C_2(h)C_3(u), \tag{66}$$

where C_1 is as in (62), while the spatial and temporal difference models, C_2 and C_3 involved in the product, are given below

$$C_2(h) = 1.3 \cdot exp\left[-(0.025\,h)^2\right] - 0.3 \cdot exp\left[-(0.0121\,h)^2\right], \tag{67}$$

$$C_3(u) = \frac{1.3}{3.597\,|u|^2+1} - \frac{0.3}{0.831\,|u|^2+1}. \tag{68}$$

Note that the compared spatio-temporal covariance models with negative values in (61) and (66) are characterised by the same marginals in space and time, thus they present the same behaviour near the origin and asymptotic behaviour at infinity along the spatial and temporal profiles.

Table 3
Basic statistics for complex kriging prediction errors, in terms of RMAE and RMSE, on the basis of 150 random validations subsets of 3 different sizes.

Validation set size	MAE			RMSE		
	41,866 (50%)	33,493 (40%)	25,120 (30%)	41,866 (50%)	33,493 (40%)	25,120 (30%)
Mean	0.068	0.062	0.056	0.105	0.092	0.076
Median	0.062	0.063	0.053	0.096	0.089	0.070
Std. deviation	0.017	0.011	0.011	0.034	0.023	0.019
Minimum	0.048	0.043	0.042	0.063	0.059	0.054
Maximum	0.108	0.076	0.083	0.175	0.130	0.120
25th percentile	0.056	0.053	0.050	0.080	0.072	0.064
75th percentile	0.076	0.071	0.063	0.129	0.107	0.085

Even this alternative spatio-temporal covariance model provides a close match to the empirical covariance, evidenced by the mean deviation between the sample and the theoretical covariance surfaces and the analogous mean squared deviation which do not show significant differences with respect to the same indexes determined for the first model. Indeed, the p-value of the test statistic computed to verify the hypothesis that the means do not differ are 0.913 and 0.954.

Moreover, the relative (absolute and squared) error indexes, computed for the cross-validation estimates and for the jackknife ones, are 0.06 and 0.13, thus they confirm its good performance in terms of estimation accuracy.

6.3. Numerical analysis for model reliability assessment

A numerical study has been carried out to assess the consistency of the proposed spatio-temporal covariance model that admits negative values. Estimation reliability has been examined as a function of size of the validation sets by using 150 subsets drawn from the original dataset. These subsets were organised into three groups of 50: the first group of validation sets composed by 41,866 (approximately 50% of the available data), the second group of validation sets composed by 33,493 (approximately 50% of the available data) and the third group of validation sets composed by 25,120 (approximately 30% of the available data). For each subset, ordinary kriging has been applied to infer on the validation points from the remaining observed values, employing the spatio-temporal covariance models in (61). Estimation errors have been summarised by the relative mean absolute error (RMAE) and the relative mean squared error (RMSE). Basic statistics for RMAE and RMSE are reported in Table 3 and indicate satisfactory model reliability. The mean RMAE decreases from 0.068 for the largest validation sets to 0.056 for the smallest, corresponding to an improvement of at least 18% as size decreases. RMSE displays a similar trend and the reduction in precision for bigger validation sets remains within acceptable bounds.

An inferential analysis on the estimation errors has also been performed to further evaluate the model's capacity to recover observed values. The null hypothesis that the mean deviation between empirical and predicted values is zero has not been rejected (p-values range from 0.79 to 0.93). Thus, both the low RMAE and RMSE values and the inferential results support the applicability and robustness of the fitted spatio-temporal covariance functions for describing the space–time dependence structure.

Remark. This application represents a typical example of a phenomenon with a spatio-temporal evolution characterised by negative correlation at least in one of the two domains of interest. In particular, in the specific application, the relationships among the data values (for a fixed time point) become discordant as the spatial lag increases, so that the corresponding spatial correlation measure is negative, while the temporal part decays monotonically and is always positive. Notably, the spatial correlation with negative values reflects pairs of locations at these lags that combine urban centres with a high ratio of internal migration with considerably neighbouring municipalities characterised by a low migration index. The negative spatial correlation at these lags likely stems from systematic differences between large urban centres and their smaller neighbouring municipalities. Indeed, large cities tend to concentrate jobs, services and transport hubs, producing high inward and outbound mobility and positive migration, while surrounding small towns show limited local opportunities and lower or negative migration levels. Pairs which combine a high-migration urban core with a low-migration periphery, produce negative correlation. Aggregation and scale effects (e.g., differences in population size, commuting catchments and functional roles) amplify this contrast, making the pattern a recurrent feature across areas with similar urban–rural structures.

The same pattern appears in datasets referred to various demographic variables, such as population density or crime distribution, or to the IMR variable in other territories, suggesting it is a very common characteristic.

7. Conclusions

Recent scientific developments produced broader classes of covariance functions obtained as differences of two correlation models; these constructions offer properties that contrast with traditional hole-effect models and yield greater adaptability. Their main limitation is that they were referred essentially to the purely spatial settings. This paper provided some further advances of the state of the art by proposing a new strategy to build spatio-temporal correlation models that can accommodate negative correlation while preserving admissibility and modelling flexibility. The presented classes of covariance functions address several of the classical limitations and extends difference-based ideas into the spatio-temporal domain. Some examples and the application shown here illustrated the practical relevance of the approach as well as its suitability to produce covariance models with negative values for higher-dimensional Euclidean domains.

Moreover, the case study focused on a spatio-temporal phenomenon that exhibits negative correlation in at least one domain of interest. Specifically, for a given time the relationships among observations become increasingly discordant as spatial lag grows, yielding a negative spatial correlation, whereas the temporal component decays monotonically and remains positive. The negative spatial correlation at these lags likely arises because large urban centres and their nearby smaller municipalities exhibit systematically different migration dynamics. Urban cores typically attract and generate substantial internal migration due to greater employment, services and connectivity, whereas surrounding towns show lower migration activity. When a high-migration city pairs with a low-migration neighbour, their migration measures tend to move in opposite directions, producing negative correlation. Differences in population size, commuting catchment areas and functional roles amplify these contrasts and make the pattern consistent across similar territories.

Further developments might regard some computational aspects associated to the fitting procedure as well as to the uncertainty quantification in the fitted parameters which merits an appropriate study.

Funding

This research was partially supported by the National Biodiversity Future Center-NBFC, Spoke 4, Activity 4.1, sub activity 4.1.1. **Funder**: Project funded under the National Recovery and Resilience Plan (NRRP), Mission 4 Component 2 Investment 1.4 - Call for tender No. 3138 of 16 December 2021, rectified by Decree n.3175 of 18 December 2021 of Italian Ministry of University and Research funded by the European Union – Next GenerationEU.

Declaration of competing interest

The authors have no competing interests to declare that are relevant to the content of this article.

Acknowledgement

We would like to express our gratitude to Editor and the reviewers for their valuable comments and suggestions which helped to improve the paper.

Appendix A. Proof of Theorem 3.1

Given the continuous, bounded, symmetric and integrable function $C(\mathbf{h},u)$ defined on $\mathbb{R}^d \times \mathbb{R}$, it is a space–time covariance function if and only if the d-variate Fourier transform $C_{\boldsymbol{\omega}}(u)$ (obtained from the partial Fourier inversion of $C(\mathbf{h},u)$, with respect to $\mathbf{h}$ in the factor space $\mathbb{R}^d$

$$C_{\boldsymbol{\omega}}(u) = \int_{\mathbb{R}^d} e^{-i\cdot\mathbf{h}^T\boldsymbol{\omega}}[AC_1(\mathbf{h},u) - BC_2(\mathbf{h},u)]d\mathbf{h}, \tag{69}$$

or equivalently $C_{\boldsymbol{\omega}}(u) = A\cdot C_{1\boldsymbol{\omega}}(u) - B\cdot C_{2\boldsymbol{\omega}}(u)$ is a covariance function for almost all $\omega \in \mathbb{R}^d$ (Cressie and Huang, 1999; Gneiting, 2002b). Consequently, given two continuous, bounded, symmetric and integrable functions $C_1(\mathbf{h},u)$ and $C_2(\mathbf{h},u)$ defined on $\mathbb{R}^d \times \mathbb{R}$, their linear combination $C(\mathbf{h},u) = A\cdot C_1(\mathbf{h},u) - B\cdot C_2(\mathbf{h},u)$, as in (13), holds the same properties. Assuming that $C_{1\boldsymbol{\omega}}(u)$ and $C_{2\boldsymbol{\omega}}(u)$ are d-variate Fourier transform s as in (15), the corresponding partial Fourier transform of the linear combination $C(\mathbf{h},u)$ in (13) is obtained through the same linear combination of the functions $C_{1\boldsymbol{\omega}}(u)$ and $C_{2\boldsymbol{\omega}}(u)$

$$C_{\boldsymbol{\omega}}(u) = \int_{\mathbb{R}^d} e^{-i\cdot\mathbf{h}^T\boldsymbol{\omega}}[A\cdot C_1(\mathbf{h},u) - B\cdot C_2(\mathbf{h},u)]d\mathbf{h} = A\cdot C_{1\boldsymbol{\omega}}(u) - B\cdot C_{2\boldsymbol{\omega}}(u), \tag{70}$$

Then, the linear combination of two continuous, bounded, symmetric and integrable functions in (13), is a space–time covariance function if and only if the linear combination $A\cdot C_{1\boldsymbol{\omega}}(u) - B\cdot C_{2\boldsymbol{\omega}}(u)$ is a correlation function for almost all $\boldsymbol{\omega}$. □

Appendix B. Proof. Theorem 4.1

Given two spatio-temporal covariance models C_1 and C_2 of type (27) in $\mathbb{R}^2 \times \mathbb{R}$, with parameters a_1, c_1 and a_2, c_2, respectively, then for a fixed u, the corresponding d-variate Fourier transforms $C_{1\boldsymbol{\omega}}(u)$ and $C_{2\boldsymbol{\omega}}(u)$ are defined through the integral in (21) and are explicitly written as follows:

$$C_{k\omega}(u) = \frac{1}{2\pi\Gamma(1)}\int_0^{\infty} \Lambda_2(\omega h)h\frac{1}{(a_k|u|^2+1)}\cdot exp\left(-\frac{c_k\,h}{(a_k|u|^2+1)^{1/2}}\right)dh =$$

$$= \frac{c_k}{(a_k|u|^2+1)^{3/2}}\cdot\frac{1}{2\pi\left(\omega^2+\frac{c_k^2}{a_k|u|^2+1}\right)^{3/2}} = \frac{c_k}{2\pi}\cdot\frac{1}{\left[(a_k|u|^2+1)\omega^2+c_k^2\right]^{3/2}}, \quad k=1,2.$$

Note that for the integral solution, the readers can refer to Gradshteyn and Ryzhik (2007).

According to Corollary 4.1, the difference $C(h,u) = A \cdot C_1(h,u) - B \cdot C_2(h,u)$, is a class of covariance functions in $\mathbb{R}^2 \times \mathbb{R}$ if and only if the weighted difference of the corresponding Fourier transforms, for a fixed u, $C_{1\omega}(u)$ and $C_{2\omega}(u)$,

$$C_\omega(u) = A \cdot \frac{c_1}{2\pi} \cdot \frac{1}{\left[(a_1|u|^2+1)\omega^2 + c_1^2\right]^{3/2}} - B \cdot \frac{c_2}{2\pi} \cdot \frac{1}{\left[(a_2|u|^2+1)\omega^2 + c_2^2\right]^{3/2}}, \tag{71}$$

is a covariance function for all ω.

By recalling the admissibility condition for the difference of rational models given in Theorem 3.3 in De Iaco and Posa (2025), given two isotropic rational covariance functions, C_1 and C_2, defined on $\mathbb{R}^d$, which are characterised by the scale parameters α and β, respectively, the following function C obtained through the weighted difference between C_1 and C_2

$$C(x;\mathbf{V}) = \frac{A_1}{(x^2+\alpha^2)^{(m+1)/2}} - \frac{B_1}{(x^2+\beta^2)^{(m+1)/2}}, \tag{72}$$

with $x = \|\boldsymbol{x}\|$, $\boldsymbol{x} \in \mathbb{R}^m$, $m \in \mathbb{N}_+$, $\mathbf{V} = (A_1, B_1, \alpha, \beta)$ and $A_1, B_1, \alpha, \beta > 0$, is a family of admissible isotropic covariance models in $\mathbb{R}^m$ for any $m \in \mathbb{N}_+$ if and only if the condition specified below:

$$\beta \geq \alpha \quad \text{and} \quad \frac{B_1}{A_1} \leq \frac{\beta}{\alpha}, \tag{73}$$

is satisfied. Then, for model (71), the domain dimension is one ($m = 1$) and the specific parameter vector is

$$\mathbf{V}' = \left(\frac{A \cdot c_1}{2\pi\left(\omega^2 a_1\right)^{3/2}}, \frac{B \cdot c_2}{2\pi\left(\omega^2 a_2\right)^{3/2}}, \sqrt{\frac{\omega^2 + c_1^2}{\omega^2 a_1}}, \sqrt{\frac{\omega^2 + c_2^2}{\omega^2 a_2}} \right).$$

By comparing the vectors $\mathbf{V}$ and $\mathbf{V}'$, the following parametric inequalities for the function in (71) have to be satisfied for all ω:

$$\sqrt{\frac{\omega^2 + c_2^2}{\omega^2 a_2}} \geq \sqrt{\frac{\omega^2 + c_1^2}{\omega^2 a_1}}, \tag{74}$$

and

$$\frac{Bc_2}{Ac_1} \cdot \left(\frac{a_1}{a_2}\right)^{3/2} \leq \sqrt{\frac{(\omega^2 + c_2^2)a_1}{(\omega^2 + c_1^2)a_2}}. \tag{75}$$

The first inequality can also be expressed as

$$\frac{\omega^2 + c_2^2}{\omega^2 + c_1^2} \geq \frac{a_2}{a_1}, \tag{76}$$

where the equality is only met if $c_1 = c_2$ for all ω, which also implies $\frac{a_2}{a_1} \leq 1$.

The second inequality in (75) can also be written as

$$\frac{c_2}{c_1} \cdot \frac{a_1}{a_2} \leq \frac{A}{B}\sqrt{\frac{(\omega^2 + c_2^2)}{(\omega^2 + c_1^2)}}, \tag{77}$$

where the equality is only met if $c_1 = c_2$ for all ω, which also implies $\frac{a_1}{a_2} \leq \frac{A}{B}$.

Note that if $c_1 \neq c_2$, the functional analysis can be conducted for the following strict inequalities:

$$\frac{\omega^2 + c_2^2}{\omega^2 + c_1^2} > \frac{a_2}{a_1}, \qquad \frac{c_2}{c_1} \cdot \frac{a_1}{a_2} < \frac{A}{B}\sqrt{\frac{(\omega^2 + c_2^2)}{(\omega^2 + c_1^2)}}. \tag{78}$$

Consequently,

- when $a_1 > a_2$ and $c_1 > c_2$, the first inequality in (78) is met if,

$$\left(\frac{c_2}{c_1}\right)^2 > \frac{a_2}{a_1}, \tag{79}$$

  while the second one in (78) is satisfied, if

$$\frac{c_2}{c_1}\frac{a_1}{a_2} < \frac{A}{B}\frac{c_2}{c_1}, \quad \Rightarrow \quad \frac{a_1}{a_2} < \frac{A}{B}. \tag{80}$$

  Thus, $1 < \left(\frac{c_2}{c_1}\right)^2 < \frac{a_1}{a_2} < \frac{A}{B}$.
- when $a_1 > a_2$ and $c_2 > c_1$, the first inequality in (78) is always met, while the second one in (78), is satisfied if

$$1 < \frac{c_2}{c_1}\frac{a_1}{a_2} < \frac{A}{B}; \tag{81}$$

- when $a_1 > a_2$ and $c_1 = c_2$, the inequalities in (78) are met if $1 < \frac{a_1}{a_2} \le \frac{A}{B}$;
- when $a_1 = a_2$ and $c_2 > c_1$, the condition (81) has to be satisfied and reduces to

$$1 < \frac{c_2}{c_1} < \frac{A}{B}, \tag{82}$$

while if $a_1 = a_2$ and $c_1 > c_2$, the admissibility conditions are never met. Of course, if $a_1 = a_2$ and $c_1 = c_2$, it is enough that $A/B \ge 1$;
- when $a_1 < a_2$, for any choice of c_1 and c_2, the first inequality in (78) is never verified.

Thus, the proof is completed. □

Note that, in a spatio-temporal domain $\mathbb{R}^d \times \mathbb{R}$, the model in (28), where C_1 and C_2 are spatio-temporal covariance models of type (27), can be explicitly written as follows:

$$C(h,u) = \frac{A}{(a_1\,|u|^2+1)^{d/2}} \cdot exp\left(-\frac{c_1\,h}{(a_1\,|u|^2+1)^{1/2}}\right) - \frac{B}{(a_2\,|u|^2+1)^{d/2}} \cdot exp\left(-\frac{c_2\,h}{(a_2\,|u|^2+1)^{1/2}}\right). \tag{83}$$

For this model, the weighted difference $C_\omega(u)$ of the corresponding Fourier transforms, for a fixed u, $C_{1\omega}(u)$ and $C_{2\omega}(u)$, can be expressed as follows:

$$C_\omega(u) = A \cdot \frac{c_1}{2\pi} \cdot \frac{1}{\left[(a_1\,|u|^2+1)\omega^2 + c_1^2\right]^{(d+1)/2}} - B \cdot \frac{c_2}{2\pi} \cdot \frac{1}{\left[(a_2\,|u|^2+1)\omega^2 + c_2^2\right]^{(d+1)/2}}; \tag{84}$$

since the d–variate spectral density of the two covariance models C_k, $k = 1,2$, of type (27), with parameters a_k, c_k for a fixed u, is obtained as follows:

$$C_{k\omega}(u) = \frac{1}{2^{d-1}(\pi)^{d/2}\Gamma(d/2)} \int_0^\infty \Lambda_d(\omega h) h^{d-1} \frac{1}{(a_k|u|^2+1)^{d/2}} \cdot exp\left(-\frac{c_k\,h}{(a_k|u|^2+1)^{1/2}}\right) dh =$$

$$= \frac{c_k}{(a_k|u|^2+1)^{d/2}(a_k|u|^2+1)^{1/2}} \cdot \frac{1}{2\pi\left(\omega^2 + \frac{c_k^2}{a_k|u|^2+1}\right)^{(d+1)/2}} =$$

$$= \frac{c_k}{2\pi} \cdot \frac{1}{\left[(a_k|u|^2+1)\omega^2 + c_k^2\right]^{(d+1)/2}}.$$

Thus, in a spatio-temporal domain $\mathbb{R}^d \times \mathbb{R}$, for any spatial dimension d, the admissibility conditions of the weighted difference in (83) can be derived, by means of a parametric study, from the conditions given on the difference of Matérn families in Posa (2025a).

Appendix C. Proof. Theorem 4.2

Given two spatio-temporal covariance models C_1 and C_2 of type (34) in $\mathbb{R}^d \times \mathbb{R}$, with parameters a_1, c_1 and a_2, c_2, respectively, then for a fixed u, the corresponding d-variate spectral density $C_{1\omega}(u)$ and $C_{2\omega}(u)$ can be explicitly obtained through the integral in (21), that is

$$C_{k\omega}(u) = \frac{1}{2^{d-1}(\pi)^{d/2}\Gamma(d/2)} \int_0^\infty \Lambda_d(\omega h) h^{d-1} \frac{1}{(a_k|u|^2+1)^{d/2}} \cdot exp\left(-\frac{c_k\,h^2}{(a_k|u|^2+1)}\right) dh =$$

$$= \frac{1}{(a_k|u|^2+1)^{d/2}} \cdot exp\left(-\frac{\omega^2(a_k|u|^2+1)}{4c_k}\right) \frac{(a_k|u|^2+1)^{d/2}}{(4\pi c_k)^{d/2}} =$$

$$= \frac{1}{(4\pi c_k)^{d/2}} \cdot exp\left(-\frac{\omega^2(a_k|u|^2+1)}{4c_k}\right), \quad k = 1,2.$$

The closed forms of the above integrals can be found in the book of Gradshteyn and Ryzhik (2007).

According to Corollary 4.1, the difference $C(h,u) = AC_1(h,u) - BC_2(h,u)$, is a class of covariance functions in $\mathbb{R}^d \times \mathbb{R}$ if and only if the weighted difference of the corresponding Fourier transforms, for a fixed u, $C_{1\omega}(u)$ and $C_{2\omega}(u)$, that is

$$C_\omega(u) = \frac{A}{(4\pi c_1)^{d/2}} \cdot exp\left(-\frac{\omega^2(a_1|u|^2+1)}{4c_1}\right) - \frac{B}{(4\pi c_2)^{d/2}} \cdot exp\left(-\frac{\omega^2(a_2|u|^2+1)}{4c_2}\right), \tag{85}$$

is a covariance function for all ω.

By recalling the admissibility condition for the difference of Gaussian models given in Theorem 3.1 of De Iaco and Posa (2025), given two isotropic Gaussian covariance functions, C_1 and C_2, defined on $\mathbb{R}^d$, which are characterised by the scale parameters α and β, respectively, the following function C obtained through the weighted difference between C_1 and C_2

$$C(x;\mathbf{V}) = A_1 \cdot e^{-\alpha x^2} - B_1 \cdot e^{-\beta x^2}, \tag{86}$$

with $x = \|\boldsymbol{x}\|$, $\boldsymbol{x} \in \mathbb{R}^m$, $m \in \mathbb{N}_+$, $\mathbf{V} = (A_1, B_1, \alpha, \beta)$, and $A_1, B_1, \alpha, \beta > 0$, is a family of admissible isotropic covariance models in $\mathbb{R}^m$ for any $m \in \mathbb{N}_+$ if and only if the following relationship,

$$1 \le \alpha/\beta \le (A_1/B_1)^{2/m}, \tag{87}$$

is respected. Then, for the model in (85), the domain dimension is one ($m = 1$) and the parameter vector is

$$\mathbf{V}' = \left(\frac{A}{(4\pi\, c_1)^{d/2}} \cdot exp\left[-\frac{\omega^2}{4c_1} \right], \frac{B}{(4\pi\, c_2)^{d/2}} \cdot exp\left[-\frac{\omega^2}{4c_2} \right], \frac{\omega^2 a_1}{4\, c_1}, \frac{\omega^2 a_2}{4\, c_2} \right)$$

By comparing the vectors $\mathbf{V}$ and $\mathbf{V}'$, the following parametric inequality for the function in (85) has to be satisfied for all ω:

$$1 \le \frac{a_1 c_2}{a_2 c_1} \le \left\{ \frac{A}{B} \left(\frac{c_2}{c_1} \right)^{d/2} exp\left[\frac{\omega^2}{4} \left(\frac{1}{c_2} - \frac{1}{c_1} \right) \right] \right\}^{2/m}, \tag{88}$$

which is met,

- when $a_1 > a_2$ and $c_1 > c_2$, if
$$1 < \frac{a_1 c_2}{a_2 c_1} \le \left(\frac{A}{B} \right)^{2/m} \left(\frac{c_2}{c_1} \right)^d \quad \Leftrightarrow \quad \left(\frac{c_1}{c_2} \right)^d < \frac{a_1}{a_2} \left(\frac{c_1}{c_2} \right)^{d-1} \le \left(\frac{A}{B} \right)^{2/m};$$
- when $a_1 \ge a_2$ and $c_1 = c_2$, if
$$1 \le \frac{a_1}{a_2} \le \left(\frac{A}{B} \right)^{2/m}.$$

Note that $a_1 = a_2$ is only admissible when $c_1 = c_2$; more generally, it can be easily shown the inequality in (88) is never met:

- for any values of a_1 and a_2, when $c_1 < c_2$;
- for $a_1 \le a_2$ and any values of c_1 and c_2, with $c_1 \ne c_2$.

Assuming that for the temporal domain $m = 1$, the proof is completed. □

References

Alegria, A., Emery, X., 2024. Matrix-valued isotropic covariance functions with local extrema. J. Multivar. Anal. 200, 105250.
Alegria, A., Emery, X., 2026. Versatile parametric classes of covariance functions that interlace anisotropies and hole effects. Stat. Sin. 36, 127–146.
Asghari, O., 2015. Geostatistical simulation of dyke systems in sungun porphyry copper deposit, Iran. J. Min. Environ. 6 (1), 1–10.
Bochner, S., 1959. Lectures on Fourier Integrals. Princeton University Press, Colorado, USA, p. 333.
Chilès, J., Delfiner, P., 1999. Geostatistics. Wiley, New York, p. 687.
Cressie, N., Huang, H., 1999. Classes of nonseparable, spatio-temporal stationary covariance functions. J. Am. Stat. Ass. 94 (448), 1330–1340.
De Cesare, L., Myers, D., Posa, D., 2001. Estimating and modeling space-time correlation structures. Stat. Probab. Lett. 51 (1), 9–14.
De Iaco, S., Hristopulos, D.T., Lin, G., 2022. Statistical deep learning for spatial and spatiotemporal data. Math. Geosci. 54, 459–465.
De Iaco, S., Myers, D., Posa, D., 2001. Space-time analysis using a general product-sum model. Stat. Probab. Lett. 52 (1), 21–28.
De Iaco, S., Myers, D., Posa, D., 2002. Nonseparable space-time covariance models: Some parametric families. Math. Geol. 34 (1), 23–41.
De Iaco, S., Palma, M., Posa, D., 2026. On the use of difference-based covariance models. Stat. Method. Appl. 35, 181–205.
De Iaco, S., Posa, D., 2018. Strict positive definiteness in geostatistics. Stoch. Env. Res. Risk Assess. 32, 577–590.
De Iaco, S., Posa, D., 2025. Characteristics of some isotropic covariance models with negative values. Spatial Stat. 68, 100905.
Gneiting, T., 2002a. Compactly supported correlation functions. J. Multivar. Anal. 83, 493–508.
Gneiting, T., 2002b. Nonseparable, stationary covariance functions for space-time data. J. Am. Stat. Ass. 97 (458), 590–600.
Gneiting, T., Sasvári, Z., Schlather, M., 2001. Analogies and correspondences between variograms and covariance functions. Adv. Appl. Prob. 33 (3), 617–630.
Gradshteyn, I.S., Ryzhik, I.M., 2007. Tables of Integrals, Series and Products. Academic Press, New York, p. 1171.
Gregori, P., Porcu, E., Mateu, J., Sasvári, Z., 2008. On potentially negative space time covariances obtained as sum of products of marginal ones. Ann. Inst. Stat. Math. 60, 865–882.
Hristopulos, D.T., Elogne, S.N., 2007. Analytic properties and covariance functions for a new class of generalized Gibbs random fields. IEEE Trans. Inf. Theory 53 (12), 4667–4679.
Johnson, S.G., 2007. The NLopt nonlinear-optimization package. https://github.com/stevengj/nlopt.
Journel, A.J., Froidevaux, R., 1982. Anisotropic hole-effect modeling. Math. Geol. 14 (3), 217–239.
Kolovos, G., Christakos, G., Hrisopoulos, D., Serre, M., 2004. Methods for generating non-separable spatiotemporal covariance models with potential environmental applications. Adv. Water Resour. 27, 815–830.
Lan, S., 2022. Learning temporal evolution of spatial dependence with generalized spatiotemporal gaussian process models. 23, (1).
Levinson, S.J., Beall, J.M., Powers, E.J., Bengtson, R.D., 1984. Space-time statistics of the turbulence in a tokamak edge plasma. Nucl. Fusion 24, 527–540.
Ma, C., 2002. Spatio-temporal covariance functions generated by mixtures. Math. Geol. 34 (8), 965–975.
Ma, C., 2005. Linear combinations of space-time covariance functions and variograms. IEEE Trans. Signal Process. 53 (3), 857–864.
Ma, Y.Z., Jones, T.A., 2001. Modeling hole-effect variograms of lithology-indicator variables. Math. Geol. 33 (5), 631–648.
Matérn, B., 1980. Spatial Variation, second ed. In: Lecture Notes in Statistics, Springer Verlag, New York, 151 p. Vol 36. 1st ed 1960 published in Meddelanden fran Statens Skogsforskningsinstitute Swed., 49(5).
Nag, P., Sun, Y., Reich, B.J., 2023. Spatio-temporal DeepKriging for interpolation and probabilistic forecasting. Spatial Stat. 57, 100773.
Pomeroy, J.W., Toth, B., Granger, R.J., Hedstrom, N.R., Essery, R.L.H., 2003. Variation in surface energetics during snowmelt in a subarctic mountain catchment. J. Hydrometeorol. 4, 702–719.

Porcu, E., Zastavnyi, V., 2011. Characterization theorems for some classes of covariance functions associated to vector valued random fields. J. Multivar. Anal. 102 (9), 1293–1301.
Posa, D., 2021. Models for the difference of continuous covariance functions. Stoch. Env. Res. Risk Assess. 35, 1369–1386.
Posa, D., 2023a. Revised and wider classes of isotropic space-time covariance functions. Stoch. Env. Res. Risk Assess. 37, 4941–4962.
Posa, D., 2023b. Special classes of isotropic covariance functions. Stoch. Env. Res. Risk Assess. 37, 1615–1633.
Posa, D., 2025a. Covariance models through the difference between Matérn families. Stoch. Env. Res. Risk Assess. 37, 1615–1633.
Posa, D., 2025b. Further advances on isotropic correlation models with negative values. Stoch. Env. Res. Risk Assess. 39, 5713–5736.
Posa, D., 2025c. Some peculiar families of correlation functions. Spatial Stat. 69, 100915.
Posa, D., De Iaco, S., Palma, M., 2025. New families of isotropic covariance functions. In: Azevedo, L., Narciso, J., Soares, A., Pereira, M.J., Vargas-Guzmán, J.A. (Eds.), International Geostatistics Congress 2024. Springer Nature Switzerland, Cham, pp. 57–64. http://dx.doi.org/10.1007/978-3-031-92870-3_6.
Rasmussen, C.E., Williams, C.K.I., 2005. Gaussian Processes for Machine Learning. The MIT Press, Massachusetts.
Rodrigues, A., Diggle, P., 2010. A class of convolution-based models for spatio-temporal processes with non-separable covariance structure. Scand. J. Stat. 37 (4), 553–567.
Shkarofsky, I.P., 1968. Generalized turbulence space-correlation and wave- number spectrum-function pairs. Can. J. Phys. 46, 2133–2153.
Vecchia, A.V., 1988. Estimation and model identification for continuous spatial processes. J. R. Stat. Soc. Ser. B Stat. Methodol. 50 (2), 297–312.
Wang, Q., Parker, P.A., Lund, R., 2025. Spatial deep convolutional neural networks. Spatial Stat. 66, 100883.
Wikle, C.K., Zammit-Mangion, A., 2023. Statistical deep learning for spatial and spatiotemporal data. Annu. Rev. Stat. Appl. 10, 247–270.
Xu, Z.W., Wu, J., Huo, W.P., Wu, Z.S., 2003a. Temporal skewness of electromagnetic pulsed waves propagating through random media with embedded irregularity slab. Chin. Phys. Lett. 20, 370–373.
Xu, Z.W., Wu, J., Wu, Z.S., 2003b. Statistical temporal behaviour of pulse wave propagation through continuous random media. Waves Random Media 13, 59–73.
Yaglom, A.M., 1955. Correlation theory of continuous processes and fields with applications to statistical extrapolation of time series and to turbolence theory. Doctor of Sci Dissertation, Institute of Atmosph. Phys., Acad. Sci. of the USSR, Moscow.
Yakhot, V., Orszag, S.A., She, Z.S., 1989. Space-time correlations in turbulence - kinematical versus dynamical effects. Phys. Fluids 1, 184–186.
Ye, J., Lazar, N.A., Li, Y., 2015. Nonparametric variogram modeling with hole effect structure in analyzing the spatial characteristics of fMRI data. J. Neurosci. Methods 240, 101–115.